

Transition from Three-Dimensional Anisotropic Spin Excitations to Two-Dimensional Spin Excitations by Electron Doping the FeAs-Based $\text{BaFe}_{1.96}\text{Ni}_{0.04}\text{As}_2$ Superconductor

Leland W. Harriger,¹ Astrid Schneidewind,² Shiliang Li,^{1,3} Jun Zhao,¹ Zhengcai Li,³ Wei Lu,³ Xiaoli Dong,³ Fang Zhou,³ Zhongxian Zhao,³ Jiangping Hu,⁴ and Pengcheng Dai^{1,3,5,*}

¹*Department of Physics and Astronomy, The University of Tennessee, Knoxville, Tennessee 37996-1200, USA*

²*Technische Universität Dresden, Institut für Festkörperphysik, 01062 Dresden, Germany*

³*Institute of Physics, Chinese Academy of Sciences, P.O. Box 603, Beijing 100190, China*

⁴*Department of Physics, Purdue University, West Lafayette, Indiana 47907, USA*

⁵*Neutron Scattering Science Division, Oak Ridge National Laboratory, Oak Ridge, Tennessee 37831-6393, USA*

(Received 22 April 2009; published 20 August 2009)

We use neutron scattering to study the effect of electron doping on the structural or magnetic order in BaFe_2As_2 . In the undoped state, BaFe_2As_2 exhibits simultaneous structural and magnetic phase transitions below 143 K. Upon electron doping to form $\text{BaFe}_{1.96}\text{Ni}_{0.04}\text{As}_2$, the system first displays the lattice distortion near ~ 97 K, and then orders antiferromagnetically at 91 K before developing weak superconductivity below ~ 15 K. The effect of electron doping is to reduce the c -axis exchange coupling in BaFe_2As_2 and induce quasi-two-dimensional (2D) spin excitations. These results suggest that the transition from 3D spin waves to quasi-2D spin excitations by electron doping is important for the separated structural and magnetic phase transitions in iron arsenides.

DOI: 10.1103/PhysRevLett.103.087005

PACS numbers: 74.25.Ha, 74.70.-b, 78.70.Nx

Understanding the doping evolution of spin excitations in copper oxides and iron arsenides is important because high-transition temperature (high- T_c) superconductivity arises from electron or hole doping of their antiferromagnetic (AF) parent compounds [1–8]. For undoped iron arsenides such as AFe_2As_2 ($A = \text{Ba}, \text{Sr}, \text{Ca}$) with a spin structure of Fig. 1(a) [9–11], spin waves consist of a large anisotropy gap at the AF zone center and excitations extend up to ~ 200 meV [12–16]. Upon doping to reach optimal superconductivity [4–6], the gapped spin wave excitations were replaced by a gapless continuum of scattering in the normal state and a neutron spin resonance below T_c [17–20]. Since spin fluctuations may play a crucial role in the superconductivity of iron arsenides [21–28], it is imperative to determine the doping evolution of spin dynamics of the parent compounds.

In the undoped state, BaFe_2As_2 exhibits simultaneous structural and magnetic phase transitions below $T_s = T_N = 143$ K [9]. Upon Co-doping to induce electrons onto the FeAs plane, the combined AF and structural phase transitions were split into two distinct transitions and the electronic phase diagram in the lower Co-doping region displays coexisting static AF order with the superconductivity [29,30]. Although neutron scattering experiments confirmed that the upper transition is structural and the AF order occurs at a lower temperature [31–33], it is unknown why the structural and magnetic phase transitions should be separated upon doping. More importantly, it is unclear what happens to the spin waves of BaFe_2As_2 when electrons are doped into these materials.

Since recent inelastic neutron scattering experiments were focused in the Co-doped samples where static AF order coexists with bulk superconductivity [31,33], we

chose to study lightly electron-doped $\text{BaFe}_{1.96}\text{Ni}_{0.04}\text{As}_2$ (where Ni concentration is nominal) without the influence of bulk superconductivity [Fig. 1(b)] [6]. Although resistivity on our $\text{BaFe}_{1.96}\text{Ni}_{0.04}\text{As}_2$ suggested $T_c \approx 15$ K [Fig. 1(c)], susceptibility measurement [Fig. 1(d)] showed a weak Meissner effect indicating a superconducting volume fraction of less than 0.2%. These results are consistent with the electronic phase diagram of $\text{BaFe}_{2-x}\text{Ni}_x\text{As}_2$ in Fig. 1(b), where no bulk superconductivity heat capacity anomaly was found for $x \leq 0.05$ [6]. We find that the effect of electron doping is to significantly reduce the c -axis exchange coupling and change the three-dimensional (3D) spin waves of BaFe_2As_2 into quasi two-dimensional (2D). These results suggest that the separated structural and magnetic phase transitions in $\text{BaFe}_{1.96}\text{Ni}_{0.04}\text{As}_2$ may be associated with the diminishing spin anisotropy gap and the 3D to 2D transition of the spin excitations.

Using the self-flux method [5], we grew a ~ 1 gram single crystal of $\text{BaFe}_{1.96}\text{Ni}_{0.04}\text{As}_2$ with an in-plane and out-of-plane mosaic of 1.74° and 2.20° full width at half maximum (FWHM, measured by doing rocking curves), respectively. We defined the wave vector Q at (q_x, q_y, q_z) as $(H, K, L) = (q_x a/2\pi, q_y b/2\pi, q_z c/2\pi)$ reciprocal lattice units (rlu) using the orthorhombic magnetic unit cell (space group Fmmm), where $a = 5.5$ Å, $b = 5.4$ Å, and $c = 12.77$ Å. We performed our neutron scattering experiment on the PANDA cold triple-axis spectrometer at the FRM II, TU Munchen, Germany [19]. Our sample was aligned in the $[H, 0, L]$ zone inside a closed cycle refrigerator.

Figures 1(c) and 1(d) show the resistivity and susceptibility data. The resistivity shows clear anomalies near 97 and 91 K before weak superconductivity sets in below

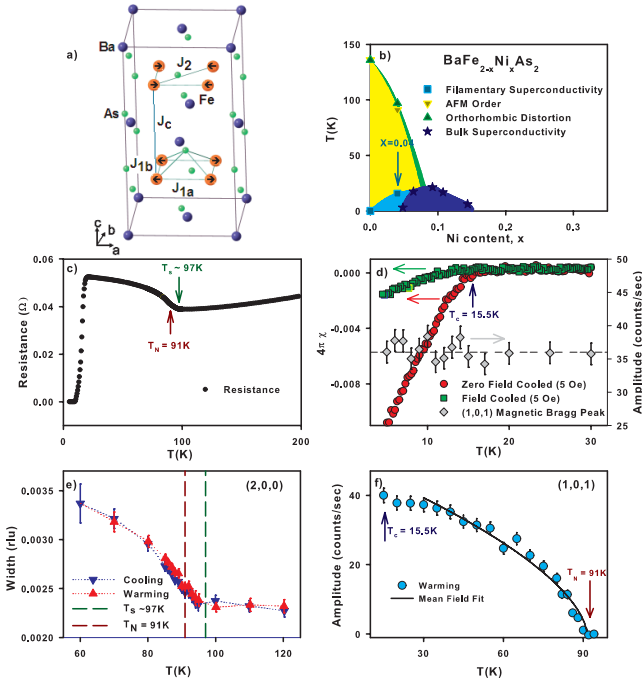


FIG. 1 (color online). (a) Diagram of the parent compound BaFe_2As_2 with Fe spin ordering and magnetic exchange couplings depicted. (b) Electronic phase diagram from Ref. [6]. (c) Temperature dependence of the resistance showing anomalies at T_s , T_N , and T_c . (d) Temperature dependence of the Meissner and shielding signals on a small crystal (field cooled $4\pi\chi = -0.001$ at 4.5 K) and the $(1, 0, 1)$ magnetic Bragg peak intensity. (e) The structural distortion of the lattice as determined by tracking the width of the $(2, 0, 0)$ nuclear Bragg peak using $\lambda/2$ scattering without Be filter. (f) Magnetic order parameter determined by Q scans around $(1, 0, 1)$ magnetic Bragg peak above background. The solid line shows order parameter fit using $(1 - T/T_N)^{2\beta}$ with $T_N = 91.3 \pm 0.7$ K and $\beta = 0.3 \pm 0.02$.

~ 15 K [Fig. 1(c)]. Similar to Co-doped BaFe_2As_2 [31–33], we find that the tetragonal to orthorhombic structural transition happens at 97 K while the AF order occurs below $T_N = 91$ K [Figs. 1(e) and 1(f)]. Therefore, the structural and magnetic phase transitions are separated immediately upon electron doping. Since $\text{BaFe}_{1.96}\text{Ni}_{0.04}\text{As}_2$ is not a bulk superconductor [Figs. 1(b) and 1(d)] [6], it is not surprising that superconductivity has negligible influence on the static AF order [Figs. 1(d) and 1(f)].

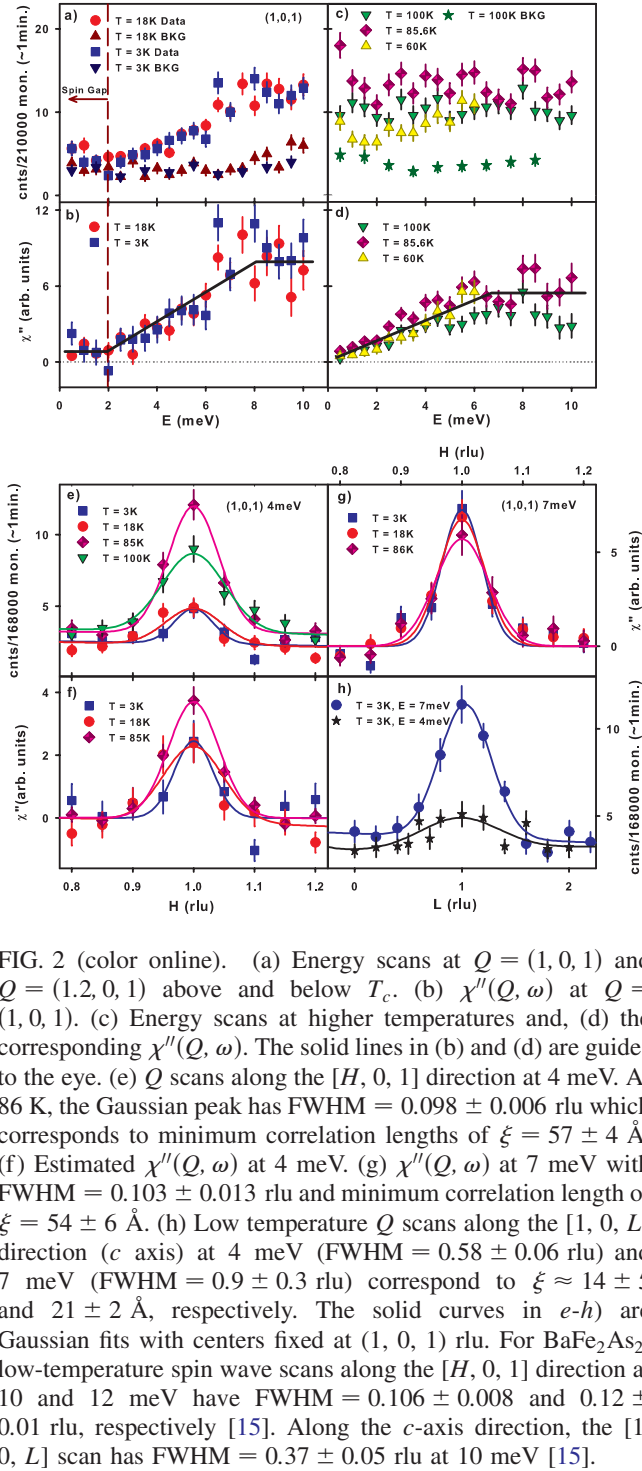
In the undoped BaFe_2As_2 , spin waves have an anisotropy gap about 8 meV at $Q = (1, 0, 1)$ [$\Delta(1, 0, 1) = 8$ meV] [13,15]. For optimally Co and Ni doped materials, spin excitations are gapless in the normal state [18,19] and superconductivity induced spin gaps open below T_c [20]. Figure 2(a) shows the constant- Q scans at the $Q = (1, 0, 1)$ (signal) and $Q = (1.2, 0, 1)$ (background) positions above and below T_c for $\text{BaFe}_{1.96}\text{Ni}_{0.04}\text{As}_2$. Figure 2(b) plots the imaginary part of the dynamic susceptibility $\chi''(Q, \omega)$ after correcting for background and Bose population factor. We find that $\chi''(Q, \omega)$ has a 2 meV normal state spin gap. Figures 2(c) and 2(d) reveal that the magnetic inten-

sity increase with increasing temperature below T_N is due mostly to the Bose population factor. These results are confirmed by Q scans along the $[H, 0, 1]$ direction at different temperatures [Figs. 2(e)–2(g)], which display well-defined peaks at $Q = (1, 0, 1)$ that have similar widths to the undoped BaFe_2As_2 at 10 meV [15]. Figure 2(h) shows Q scans along the c axis $[1, 0, L]$ direction. Fourier transforms of the wave vector scans in Figs. 2(g) and 2(h) suggest that spins are only correlated around two unit cells (~ 20 Å) along the c axis, much smaller than the 10 unit cell correlations (~ 50 Å) of in-plane spin excitations. Therefore, spin excitations in $\text{BaFe}_{1.96}\text{Ni}_{0.04}\text{As}_2$ are not entirely 2D like those of optimally Co-doped material [18].

Further evidences for quasi-2D spin excitations in $\text{BaFe}_{1.96}\text{Ni}_{0.04}\text{As}_2$ are summarized in Fig. 3. Assuming spin excitations in $\text{BaFe}_{2-x}\text{Ni}_x\text{As}_2$ can be described by an effective Heisenberg Hamiltonian, the spin anisotropy gaps at $Q = (1, 0, 1)$ and $Q = (1, 0, 0)$ are $\Delta(1, 0, 1) = 2S[(J_{1a} + 2J_2 + J_c + J_s)^2 - (J_c + J_{1a} + 2J_2)^2]^{1/2}$ and $\Delta(1, 0, 0) = 2S[(2J_{1a} + 4J_2 + J_s)(2J_c + J_s)]^{1/2}$, respectively [12,13,15,16]. Here S is the magnetic spin ($=1$); J_{1a} , J_2 , J_c are effective in-plane nearest-neighbor, next nearest-neighbor, and c -axis magnetic couplings, respectively [Fig. 1(a)]. J_s represents the magnetic single ion anisotropy. For BaFe_2As_2 , we estimate $\Delta(1, 0, 1) = 7.8$ meV and $\Delta(1, 0, 0) = 20.2$ meV assuming $J_{1a} = 36$, $J_2 = 18$, $J_c = 0.3$, $J_s = 0.106$ meV [13,15,16]. Upon electron doping to form $\text{BaFe}_{1.96}\text{Ni}_{0.04}\text{As}_2$, these spin gap values have been reduced to $\Delta(1, 0, 1) = 2$ meV and $\Delta(1, 0, 0) = 4$ meV [Figs. 2(b) and 3(b)]. Since such electron doping hardly changes the in-plane Q -scan widths compared to that of the undoped BaFe_2As_2 [Figs. 2(e)–2(g), 3(e), and 3(g)] [13,15], it should only slightly modify the in-plane exchange couplings. Assuming that J_{1a} and J_2 are unchanged in $\text{BaFe}_{1.96}\text{Ni}_{0.04}\text{As}_2$, the observed $\Delta(1, 0, 1) = 2$ meV and $\Delta(1, 0, 0) = 4$ meV would correspond to $J_c = 0.01$ meV and $J_s = 0.007$ meV, suggesting a rapid suppression of c -axis exchange coupling and magnetic single ion anisotropy with electron doping.

In Ref. [33], it was argued that spin anisotropy for $\text{BaFe}_{1.92}\text{Co}_{0.08}\text{As}_2$ is similar to that of the BaFe_2As_2 , meaning that the reduction in spin gap at $Q = (1, 0, 1)$ arises mostly from reduced J_{1a} and J_2 . Assuming the best fitted values of $S(J_{1a} + 2J_2) = 32$ meV and $SJ_c = 0.34$ meV [33], we expect $\Delta(1, 0, 1) = 5.5$ meV and $\Delta(1, 0, 0) = 14.2$ meV with $SJ_s = 0.106$ meV. These values are clearly different from the observation. Even if we assume all exchange couplings to reduce by 50% upon electron doping with $S(J_{1a} + 2J_2) = 16$ meV, $SJ_c = 0.15$ meV, and $SJ_s = 0.05$ meV, we still find $\Delta(1, 0, 1) = 3.8$ and $\Delta(1, 0, 0) = 10$ meV. This suggests that the large reduction in the $\Delta(1, 0, 0)$ gap values upon electron doping is due to the reduced J_c and 3D nature of the system.

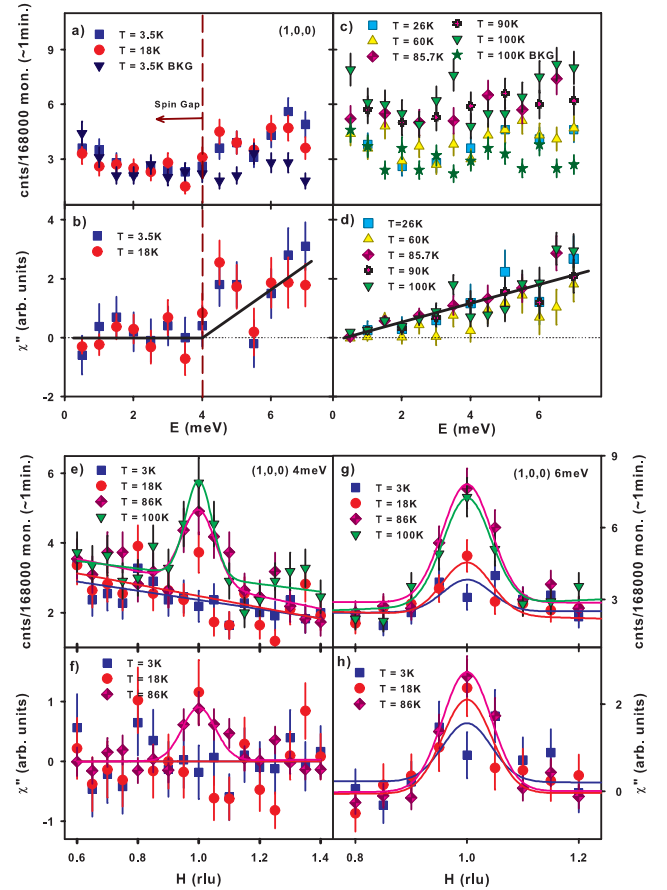
To determine the temperature dependence of $\Delta(1, 0, 0)$, we show in Fig. 3(c) the observed scattering at the signal



$Q = (1, 0, 0)$ and background $(1.4, 0, 0)$ positions at several temperatures. Figure 3(d) plots the estimated $\chi''(Q, \omega)$. Comparing Fig. 3(d) with Fig. 3(b), the 4 meV spin gap $\chi''(Q, \omega)$ at 18 K vanishes upon warming to above 60 K. These results are confirmed by Q scans at 4 meV along the $[H, 0, 0]$ direction [Fig. 3(e)]. While scans at 2 and 18 K have no obvious peaks, the scattering at 86 and 100 K shows clear peaks centered at $Q = (1, 0, 0)$. For Q scans at 6 meV, the scattering shows well-defined peaks at

all temperatures [Fig. 3(g)]. Converting these data into $\chi''(Q, \omega)$ in Fig. 3(h) confirms the results of Fig. 3(d).

Finally, we show in Fig. 4(a) the temperature dependence of the 1 meV scattering at the $Q = (1, 0, 0)$ (signal) and $Q = (1.4, 0, 0)$ (background) positions. While the background scattering only increases slightly with increasing temperature and shows no anomaly across T_N , the scattering at $Q = (1, 0, 0)$ clearly peaks at T_N . Q scans along the $[H, 0, 0]$ direction at 1 meV confirm these results [Fig. 4(c)]. Temperature dependence of the scattering at 4 meV and $Q = (1, 0, 1)$ shows similar behavior [Fig. 4(b)]. These results suggest that the disappearing $\Delta(1, 0, 1)$ and $\Delta(1, 0, 0)$ gaps near T_N arise from critical scattering associated with the static AF order.



all temperatures [Fig. 3(g)]. Converting these data into $\chi''(Q, \omega)$ in Fig. 3(h) confirms the results of Fig. 3(d).

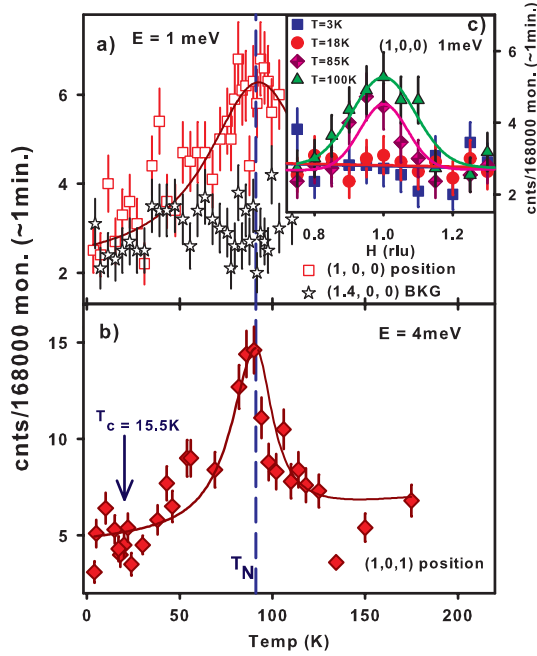


FIG. 4 (color online). (a) Temperature dependence of the 1 meV scattering at the signal $Q = (1, 0, 0)$ and background $Q = (1.4, 0, 0)$ positions. The inset shows Q scans along the $[H, 0, 0]$ at 1 meV and different temperatures. The scattering shows no anomaly across T_c but clearly peaks at T_N . (b) Temperature dependence of the scattering at 4 meV and $Q = (1, 0, 1)$ again peaks at T_N .

To understand the separated structural and magnetic phase transitions for $\text{BaFe}_{1.96}\text{Ni}_{0.04}\text{As}_2$, we note that in an effective J_1 - J_2 - J_c model [23,24], the separation of the lattice and magnetic transition temperatures is controlled by the value of J_c [23]. There is only one transition temperature when J_c is large. A finite separation between the two transition temperatures occurs when J_c/J_2 is reduced to the order of 10^{-3} . Our experimental result of $J_c/J_2 \sim 0.5 \times 10^{-3}$ is consistent with this picture. To quantitatively estimate the reduced T_N due to the smaller J_c , we note that $T_N \sim J_2/\ln(J_2/J_c)$ [23]. Let J_a^0 be the magnetic exchange values for the parental compounds, we can write $T_N^0/T_N = a[\ln(b) + \ln(c) - \ln(a)]/\ln(c)$, where $a = J_2^0/J_2$, $b = J_c^0/J_c$, $c = J_2^0/J_c^0$. Using the experimental values of the exchange coupling parameters determined earlier, we obtain $(J_2/J_2^0) = (1/a) \sim 0.87$, which is self-consistent with our suggestion that upon doping, the coupling between layers J_c is dramatically reduced while the change of the in-plane magnetic exchange coupling is small. These results provide a natural and consistent interpretation for our experimental observations.

In summary, we have shown that the most dramatic effect of electron doping in BaFe_2As_2 is to transform the 3D anisotropic spin waves into quasi-2D spin excitations. Similar dimension reduction on the electronic states of 122 materials has also been observed in angle resolved photoemission spectroscopy [34,35]. While the microscopic ori-

gin of such dimension reductions upon doping is unclear, these results suggest that reduced dimensionality in spin excitations of iron arsenides is important for the separated structural and magnetic phase transitions in these materials, and also possibly the occurrence of bulk superconductivity.

This work is supported by the U.S. NSF No. DMR-0756568, U.S. DOE BES No. DE-FG02-05ER46202, and by the U.S. DOE, Division of Scientific User Facilities. The work in IOP is supported by CAS, the MOST of China. The PANDA project of FRM II is supported by DFG within Sonderforschungsbereich 463.

*daip@ornl.gov

- [1] P. A. Lee, N. Nagaosa, and X.-G. Wen, *Rev. Mod. Phys.* **78**, 17 (2006).
- [2] R. J. Birgeneau *et al.*, *J. Phys. Soc. Jpn.* **75**, 111003 (2006).
- [3] Y. Kamihara *et al.*, *J. Am. Chem. Soc.* **130**, 3296 (2008).
- [4] M. Rotter *et al.*, *Phys. Rev. Lett.* **101**, 107006 (2008).
- [5] L. J. Li *et al.*, *New J. Phys.* **11**, 025008 (2009).
- [6] S. L. Bud'ko *et al.*, *Phys. Rev. B* **79**, 220516 (2009).
- [7] C. de la Cruz *et al.*, *Nature (London)* **453**, 899 (2008).
- [8] J. Zhao *et al.*, *Nature Mater.* **7**, 953 (2008).
- [9] Q. Huang *et al.*, *Phys. Rev. Lett.* **101**, 257003 (2008).
- [10] J. Zhao *et al.*, *Phys. Rev. B* **78**, 140504(R) (2008).
- [11] A. I. Goldman *et al.*, *Phys. Rev. B* **78**, 100506(R) (2008).
- [12] J. Zhao *et al.*, *Phys. Rev. Lett.* **101**, 167203 (2008).
- [13] R. A. Ewings *et al.*, *Phys. Rev. B* **78**, 220501(R) (2008).
- [14] R. J. McQueeney *et al.*, *Phys. Rev. Lett.* **101**, 227205 (2008).
- [15] K. Matan *et al.*, *Phys. Rev. B* **79**, 054526 (2009).
- [16] J. Zhao *et al.*, *Nature Phys.* **5**, 555 (2009).
- [17] A. D. Christianson *et al.*, *Nature (London)* **456**, 930 (2008).
- [18] M. D. Lumsden *et al.*, *Phys. Rev. Lett.* **102**, 107005 (2009).
- [19] S. Chi *et al.*, *Phys. Rev. Lett.* **102**, 107006 (2009).
- [20] Shiliang Li *et al.*, *Phys. Rev. B* **79**, 174527 (2009).
- [21] I. I. Mazin and J. Schmalian, *Physica C (Amsterdam)* **469**, 614 (2009).
- [22] J. Dai *et al.*, *Proc. Natl. Acad. Sci. U.S.A.* **106**, 4118 (2009).
- [23] C. Fang *et al.*, *Phys. Rev. B* **77**, 224509 (2008).
- [24] C. Xu *et al.*, *Phys. Rev. B* **78**, 020501 (2008).
- [25] K. Seo *et al.*, *Phys. Rev. Lett.* **101**, 206404 (2008).
- [26] F. Wang *et al.*, *Phys. Rev. Lett.* **102**, 047005 (2009).
- [27] Z. Y. Weng, arXiv:0804.3228.
- [28] A. V. Chubukov, *Physica C (Amsterdam)* **469**, 640 (2009).
- [29] N. Ni *et al.*, *Phys. Rev. B* **78**, 214515 (2008).
- [30] J.-H. Chu *et al.*, *Phys. Rev. B* **79**, 014506 (2009).
- [31] D. K. Pratt *et al.*, arXiv:0903.2833 [Phys. Rev. Lett. (to be published)].
- [32] C. Lester *et al.*, *Phys. Rev. B* **79**, 144523 (2009).
- [33] A. D. Christianson *et al.*, arXiv:0904.0767v1 [Phys. Rev. Lett. (to be published)].
- [34] V. B. Zabolotnyy *et al.*, *Physica C (Amsterdam)* **469**, 448 (2009).
- [35] C. Liu *et al.*, *Phys. Rev. Lett.* **102**, 167004 (2009).